Journal of Molecular Structure 1201 (2020) 127152

Contents lists available at ScienceDirect

Journal of Molecular Structure

journal homepage: http://www.elsevier.com/locate/molstruc

Analysis of polystyrene and polycarbonate used in manufacturing of water and food containers using laser induced breakdown spectroscopy

W.A. Farooq [a, *], Awatef S. Al-Johani [a], M.S. Alsalhi [a, b], Walid Tawfik [c], Rabia Qindeel [a]

[a] Department of Physics and Astronomy, College of Science, King Saud University, Riyadh, Saudi Arabia
[b] Research Chair in Laser Diagnosis of Cancers, College of Science, Department of Physics and Astronomy, King Saud University, Riyadh, 11451, Saudi Arabia
[c] National Institute of Laser Enhanced Sciences NILES, Cairo University, Cairo, Egypt

ARTICLE INFO

Article history:
Received 10 April 2019
Received in revised form
23 August 2019
Accepted 27 September 2019
Available online 3 October 2019

Keywords:
Laser
Spectroscopy
Polymer
Analysis

ABSTRACT

Laser-induced breakdown spectroscopy (LIBS) is one of the analytical techniques which has vast applications in the material analysis. We have applied LIBS technique for the elemental analysis to determine trace elements as impurities in polystyrene and polycarbonate polymer materials. These polymer samples were collected from one of the Saudi industries which are being used as containers for food and water. The study was carried out under high vacuum (1×10^{-5} mbar) using a 10 Hz Q-switched pulsed Nd:YAG laser at wavelength 1064 nm, 20 mJ energy and 8 ns pulse width to generate the plasma of the polymer samples. By analyzing the plasma plume emission, LIBS spectra revealed the existence of Al, Si, P, Ca, Mg, N in Polystyrene and Br, Mg, Ca, N in polycarbonate as trace elements. Molecular lines of CN, CO, C2 and CH in these samples have been observed as well. The presence of Al, Si, and P traces in these polymer samples might be harmful to the human body. LIBS is found to be a simple, non-contact, online and cost-effective method to identify the hazardous elements in polymers. The industries can adopt this method to provide harmless containers for water or food products.

1. Introduction

Laser-induced breakdown spectroscopy (LIBS) is one of the atomic emission spectroscopic analytical techniques that can be used for quantitative and qualitative analysis of any state of material [1–4]. LIBS technique involves a laser beam focused on the target to generate a plasma plume on the target surface [5,6]. Generally, atomic emission spectroscopic analytical techniques depend on emission of electromagnetic radiation from the constituents of target material after excitation of atoms, ions or molecules present in a target sample. Thus, an energy source is required in these techniques to excite the species present in the sample to higher energy states and after de-excitation, emit characteristic radiations which are collected, sent to a spectrograph and detected by various types of detectors [7–10].

LIBS is a method of atomic emission spectroscopy (AES) also sometimes called laser-induced plasma spectroscopy (LIPS) or laser spark spectroscopy (LSS) has developed rapidly as an analytical technique over the past two decades [11,12]. This technique employs a low-energy pulsed laser (typically tens to hundreds of mJ per pulse) and a focusing lens to generate plasma that vaporizes a small amount of a sample [12]. The nature of the laser-induced plasma from target depends on various parameters such as laser wavelength, pulse duration and intensity, spot size, thermal and optical properties of the sample surface and the ambient gas (vacuum, inert, air and the pressure) [13]. There has been an increasing trend in recent years towards analytical technologies that can carry out spatially resolved surface analysis for industry, nanotechnology, geology and biomedicine applications. In order to give better insight into the surface sample structure with important benefits than standard bulk analysis, the measurements which are spatially resolved are needed. The latest advances in LIBS and its easy use have enabled the creation of schemes which can perform multi-part analysis of significant and trace components in a spatial resolution of ~10 μm (or less) at rapid acquisition speeds of up to kHz per pixel [2,12]. Conventional and LIBS imagery both share the same measurement principles, but with LIBS, plasma is created in a

* Corresponding author.;
E-mail addresses: wafarooq@hotmail.com, awazirzada@ksu.edu.sa (W.A. Farooq).

https://doi.org/10.1016/j.molstruc.2019.127152
0022-2860/

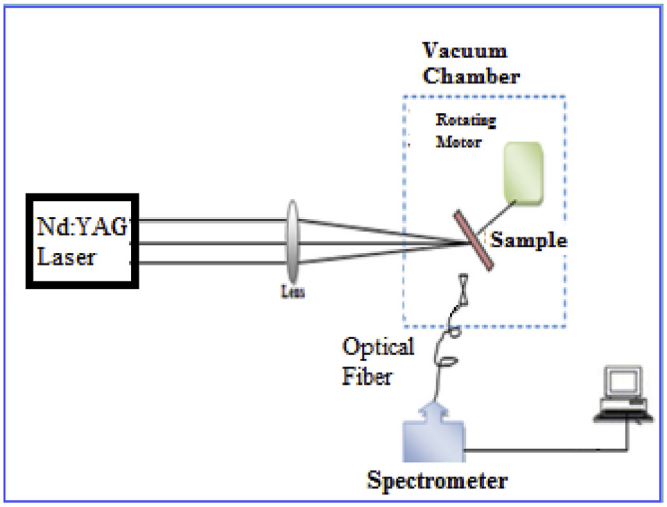

Fig. 1. Block diagram of LIBS setup in high vacuum chamber.

predefined region in distinct locations on the sample surface. The elemental maps will then be created to get a corresponding elemental image after extracting the line intensities connected with the components of concern from every recorded spectrum. LIBS with a spatial resolution has gained more attention and is now identified as the fresh axis of growth for elemental analysis. Indeed, because of its simplicity, no sample pre-treatment needed and no aggressive chemical used. LIBS offers distinctive characteristics in comparison to standardized techniques such as inductively coupled plasma mass spectrometry (ICP-MS), X-ray fluorescence (XRF), electron probe microanalysis (EPMA), and secondary ion mass spectrometry (SIMS) [12]. In addition, LIBS with a portable Echelle spectrometer and ICCD camera, can be adapted to observe lower limit of detection (LOD) for iron, beryllium, magnesium, silicon, manganese and copper as minor elements in the ppm range with high precision by following some optimization of data acquisition procedures [4].

In the present investigations we have applied LIBS technique for the elemental analysis of polystyrene, polycarbonate materials from one of the Saudi industries which are being used in manufacturing of water and food containers to find impurities and hazardous elements. The objective of the research was to identify the harmful elements present in these polymers. The experiment was performed in high vacuum chamber and a laser beam of 1064 nm wavelength from Q-switched pulsed Nd:YAG laser was focused on the target through a quartz window to generate the plasma on the sample surface placed on rotating stage in the vacuum chamber.

Polymers are organic materials. Organic materials are the materials which contain carbon atoms chemically combined with hydrogen and their structures, in most cases, are fairly complex. Thus, carbon forms the “spine” of the polymer chain, and the other constituents attach themselves to the carbon [14].

Most polymers are based on hydrocarbons, some of the simple hydrocarbons belong to the paraffin family; the chain like paraffin molecules include methane (CH_4), ethane (C_2 H_6), propane (C_3 H_8), and butane (C_4 H_10) where the elements of carbon and hydrogen form predictable combinations based on the relationship, C_n H_(2n+2). In each molecule the covalent bonds are strong, but only weak hydrogen and van der Waals bonds exist between molecules, and therefore these hydrocarbons have relatively low melting and boiling points. On the other hand, boiling temperatures rise with increasing molecular weight [15].

From LIBS spectra of the polymer samples, it was found that Al, Si, P, Ca, Mg, N in Polystyrene and Br, Mg, Ca, N in polycarbonate were present as impurities in the samples. Some molecular lines of CN, CO, C2 and CH molecules were also observed in LIBS spectra of these samples. Presence of Al, Si, and P might be harmful to the human body. LIBS technique is found to be a simple and cost-effective method to identify the hazardous elements. The industries can adopt this technique to provide harmless containers for water or food products.

2. Experimental

In order to make the samples as uniform disc for LIBS experiment following procedure was carried out.

A glass flask cleaned with chloroform then with deionizing water and then dried it by heating at 100 °C in the oven. Three grams of polycarbonate powder were put in the dried flask then a 50 ml Chloroform was added in the flask. The flask was capped and stirred using ultrasonic bath. Then the solution was poured into the glass dishes and allowed it to dry for about 2 h. The prepared discs were cut into small pieces and one piece is fixed at rotating disc in the vacuum chamber shown in Fig. 1.

The LIBS experimental setup used in the present investigation is depicted in Fig. 1. A pulse of laser beam of wavelength 1064 nm, 20 mJ energy and 8 ns pulse width from Nd:YAG laser was focused on the target material which was fixed at a rotating disc in vacuum chamber. In order to provide fresh surface of the sample for each pulse, the sample was rotated at 10 Hz using a dc motor. 10^{-5} mbar vacuum was maintained in the chamber using diffusion pump. The focused laser beam generated plasma on the surface of target material (Polystyrene or polycarbonate). After cooling in a few nanoseconds, the generated plasma emitted radiations which were collected with LM-P10 fiber optical cable and passed through spectrometer (Oriel® MS257™) equipped with ICCD camera (iStar-ANDOR). The output radiations from the spectrometer were recorded with the ICCD camera and stored in computer as LIBS spectra of the corresponding material. These LIBS spectra are signature of the elements present in the target sample.

3. Results and discussions

LIBS spectra obtained from Polystyrene (PS) and polycarbonate (PC) in the range of 200−1000 nm are depicted in Fig. 2(a) and (b) respectively. These spectra were analyzed using NIST data [16]. Spectral lines detected in PS and PC LIBS spectra are listed along with other spectral data in Table 1 and Table 2 respectively. The corresponding data of the spectral lines are taken from NIST data [16,17]. In the LIBS spectra of the samples shown in Fig. 2, some impurities are observed which are Al, Si, P, Ca, Mg, N in PS Polymer sample and Br, Mg, Ca, N in PC polymer sample. The prominent lines of the impurities detected in the samples are shown in Fig. 3(a) and Fig. 3(b) for PS and PC samples respectively. Some molecular lines of CN, CO, C2 and CH molecules are also observed in the LIBS spectra of these samples which are also depicted in Fig. 3(a and b) (see Table 3).

Plasma temperature is one of the most important parameters for the understanding of the processes occurring in the plasma. The plasma temperature is determined using Boltzmann plot. The use of Boltzmann equation for plasma temperature determination is based on the assumption that the plasma is in the state of local thermal equilibrium (LTE) and the selected spectral lines must be optically thin. In fact, complete thermal equilibrium is never reached in laboratory plasmas and equilibrium occurs in small regions of space, although it may be different from region to region,

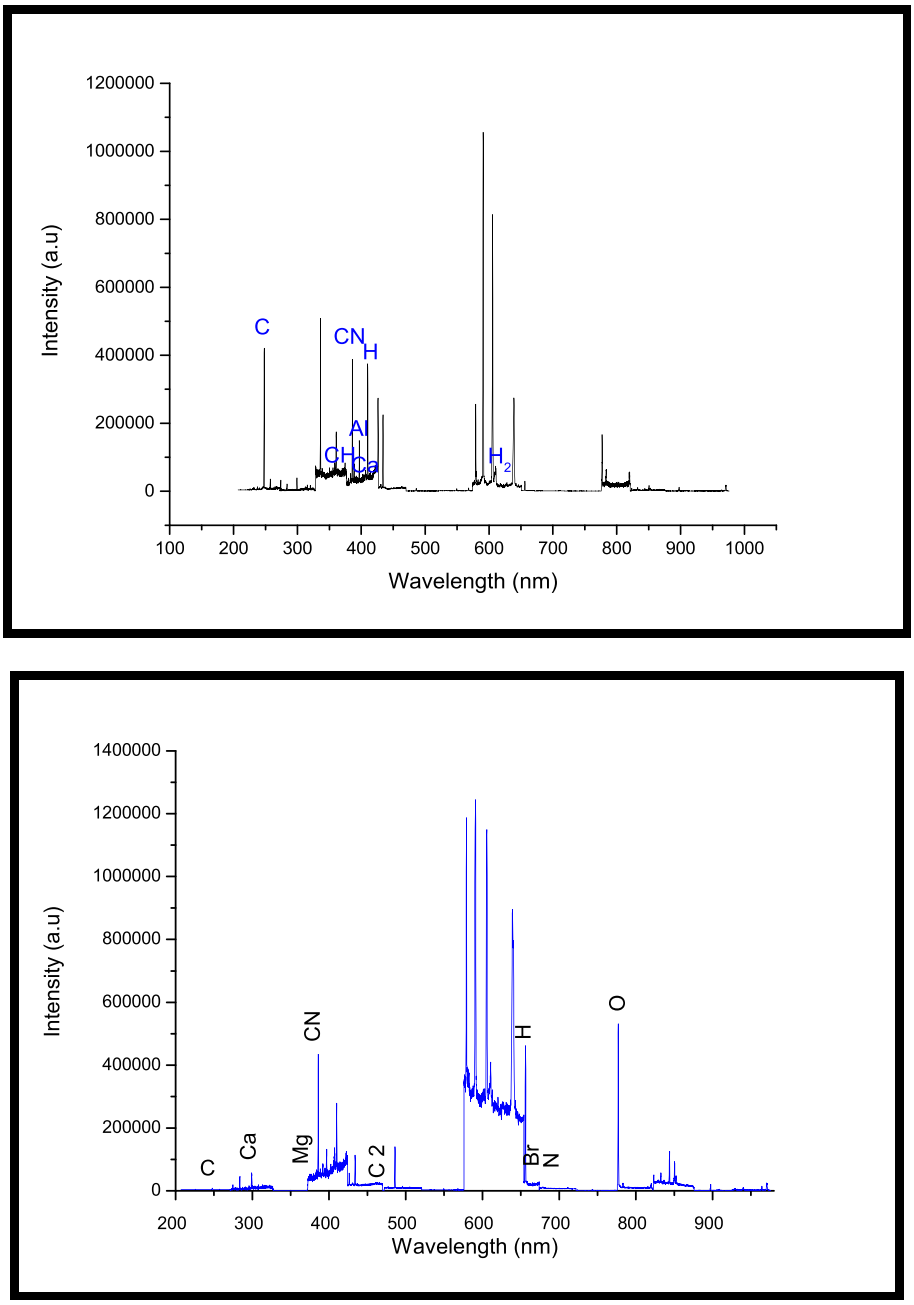

Fig. 2. (a) LIBS spectrum of PS sample from 200 nm−1000 nm. (b) LIBS spectrum of Polycarbonate from 200 nm to 1000 nm.

so it is approximated as local thermal equilibrium (LTE) whereas, the optically thin plasma means that the emission lines coming out directly from the plasma without shielding effect [18].

When the excited atoms return to their lower energy configurations by emitting photons, spectral lines corresponding to the transitions between these different levels can be observed in emission spectra. Thus, the line intensity (number of transitions per unit volume per unit time) corresponding to these transitions can be calculated by the following formula [2]:

$$\frac{I_{ki}\lambda_{ki}}{A_{ki}g_k} = \frac{hc}{4\pi}\frac{n^s}{U^s(T)}e^{-E_k/kT} \quad (1)$$

where λ_{ki} , A_{ki} and g_k are the wavelength, the transition probability from level K to i and the statistical weight for the upper level, respectively; c is the speed of light in vacuum, and h is Planck's constant. When we take the natural Logarithm of both sides of the above equation the familiar form of the Boltzmann plot equation is obtained

$$\ln\left(\frac{I_{ki}\lambda_{ki}}{A_{ki}g_k}\right) = \ln\left(\frac{hc}{4\pi}\frac{n^s}{U^s(T)}\right) - \frac{E_k}{kT} \quad (2)$$

where λ_{ki}, A_{ki} and g_k are the wavelength, the transition probability from level K to i and the statistical weight for the upper level, respectively; c is the speed of light in vacuum, and h is Planck's constant. This Boltzmann equation is used to calculate plasma temperature.

The above Boltzmann equation is identical to the equation of a straight line with slope of ((-1)/kT). Plot of the left-hand side of

Table 1
The spectroscopic data detected in analyzed spectrum of sample PS from 206 nm–976 nm.

Element	λ(*nm*)	A_{ki} g_k (S^{-1})	I (*a.u*)	E_k (cm^{-1})	E_i (cm^{-1})
Al I	877.2871	38800000	1401	43831.1	32435.45
Al I	807.6285	352000	22239	45344.17	32965.64
Al I	257.5094	216000000	36150	38933.97	112.061
Al I	270.814		10942	69880.29	32965.64
Al I	394.4006	99800000	41053	25347.76	0
Al I	396.152	197000000	149563	25347.756	112.061
Al I	783.5309	22300000	64180	45194.681	32435.453
Al II	811.965	26200000	20992	145135.3	132822.9
C II	240.2403	103000000	10206	173347.84	131735.52
C I	247.8561	84000000	421255	61981.82	21648.01
C II	392.0681	254000000	45321	157234.07	131735.52
C II	432.1657	44800000	12028	209576.46	186443.69
C I	437.1367	3810000	12791	84851.53	61981.82
C II	463.763	18300000	12419	184074.59	162517.89
C I	580.023	312000	59012	81325.76	64089.85
C I	598.64	152000	23414	86389.38	69689.48
C I	600.298	1250000	30626	86397.8	69744.03
C I	601.321	3920000	27770	86369.47	69744.03
C I	784.824	2010000	29515	84103.1	71364.9
C I	785.286	2250000	26445	84116.09	71385.38
C I	786.088	7650000	29570	84103.1	71385.38
C I	805.862	5450000	24004	83791.04	71385.38
C I	818.268	4100	25053	72610.72	60393.14
H I	410.1702	17151000	374896	106632.16205	82258.91911
H I	434.0427	31419000	224948	105291.6519	82258.91911
H I	486.1279	68752000	8877	102823.8942	82258.91911
H I	656.2725	89792000	29870	97492.3196	82258.9543
Ca I	299.4957	1.1E+08	38989	48537.62	15157.9
Ca I	314.0786	24000000	9027	47040.01	15210.06
Ca I	320.9957	22000000	7712	46301.97	15157.9
Ca I	610.2723	29000000	74303	31539.5	15157.9
Ca I	422.67	654000000	76771	23652.3	0
CH	314.49		12493		
CH	315.66		18661		
CH	362.8		60163		
CH	402.53		50632		
CH	438.5		9825		
H_2	406.688		62336		
H_2	421.25		64212		
H_2	577.505		27404		
CN	358.39		84364		
CN	386.1		388212		
CN	387.14		37627		
CN	415.24		45430		
CN	415.81		44241		
CN	450.22		10227		
CN	585.82		24831		
CN	627.19		21837		

above equation vs. E_k gives a slope of ((-1)/kT) and value of T (plasma temperature) can be calculated by measuring the slop of the line. In this experiment, the plasma temperatures were determined from the emission line intensities of the detected elements.

In Fig. 4(a) Boltzmann plots for Carbon C I, Aluminum Al I, Calcium Ca I lines observed from LIBS spectra of PS and in Fig. 4(b) Boltzmann plots for Carbon C I, Magnesium Mg I, Calcium Ca I lines observed from LIBS spectra of PC samples are shown [19]sss. The statistical weights, value of E_k and transition probabilities used to draw these plots were obtained from Kramida et al. (2014)/NIST data [16,17] and are listed in Tables (1 and 2). The slope of the curve yields a temperature of these elements which are given in Table 4 for PS and PC samples. Thus, taking average of all the temperatures of constituents of the sample, the plasma temperature of PS is 8537.7 K and for PC is 8681.26 K.

The emission spectrum reveals noticeable line broadening, which is an important parameter for the determination of the electron number density (Ne). The Stark broadens results from coulomb interactions between the radiator and the charged particles present in the plasma which is a primary mechanism influencing these emission spectra. Both ions and electrons induce Stark broadening, play a major role due to their higher velocities. The Stark broadening may be one of the reasons since the broadening effect increases with the increase of the energy level. The greater the number density of electrons greater the Stark broadening effect.

The electron number density is related to the full width at half maximum (FWHM) of Stark broadening lines. Both the linear and the quadratic Stark effect are encountered in the spectral lines. In the case of linear Stark effect (hydrogen and hydrogenic like ions) the following equation is used to calculate electron number density Ne:

$$N_e = C(N_e, T_e)\Delta\lambda^{\frac{3}{2}}_{FWHM} \quad (3)$$

where Δλ is the full width at half maximum (FWHM) and the values of the parameter C(Ne, T) which determines the relative contribution of the electron collision to the electrostatic fields weakly

Table 2
The spectroscopic data detected in analyzed spectrum of sample PC from 206 nm–976 nm.

Element	λ(*nm*)	A_{ki} g_k (S^{-1})	I (*a.u*)	E_k (cm^{-1})	E_i (cm^{-1})
Br I	444.17	3000000	21561	85937.21	63429.82
Br I	447.77	10000000	20047	85756.21	63429.82
Br I	457.57	6400000	21899	89025.04	67176.86
C I	247.8561	84000000	8385	61981.82	21648.01
C II	272.7306	26500000	6433	214430	177774.6
C I	290.327	3870000	10486	105798.7	71364.9
C II	318.35	96	14389	142027.1	110624.2
C II	318.77	324	15730	142027.1	110665.6
C I	476.2313	1010000	10941	81325.76	60333.43
C I	477.1742	3980000	13736	81343.99	60393.14
C I	601.223	1820000	322097	86317.64	69689.48
C I	602.856	337000	324524	86327.16	69744.03
C I	610.766	2080000	409845	87753.73	71385.38
C I	658.761	15300000	30525	84032.15	68856.33
C I	667.185	3340000	21003	86369.6	71385.38
C I	667.964	666000	24714	86331.63	71364.9
C I	671.132	300000	24567	83752.41	68856.33
C I	802.125	2230000	11130	83848.83	71385.38
C I	804.534	1360000	10887	83791.04	71364.9
C I	805.862	5450000	10827	83791.04	71385.38
O II	520.6651	133000000	9317	233430.5	214229.7
O I	295.8365	0.000242	16459	33792.58	0
O I	436.8193	756000	23169	99681.31	76794.98
O I	639.1733	0.0000043	895779	15867.86	226.977
O I	615.6778	35600000	287541	102865.5	86627.78
O I	465.5357	3870000	24802	108106.1	86631.45
O I	844.6247	32200000	125540	88631.3	76794.98
O I	287.6295	1470000	11141	123387.3	88630.59
O I	632.3385	54300	276820	113298.3	97488.38
O II	448.4504	116000	19618	234454.6	212161.9
O II	459.6177	500000000	22663	228723.8	206972.7
O I	798.2398	92700	11091	101155.4	88631.3
O I	799.5075	394000	11782	101135.4	88631.15
O I	777.1944	258000000	531876	86631.45	73768.2
H I	410.1702	17151000	278127	106632.2	82258.92
H I	434.0427	31419000	112733	105291.7	82258.92
H I	486.1279	68752000	139766	102823.9	82258.92
H I	656.2725	89792000	461332	97492.32	82258.95
Ca I	299.4957	1.1E+08	57695	48537.62	15157.9
Ca I	300.6861	3.8E+08	14196	48563.52	15315.94
Ca I	313.6019	12000000	16731	47036.23	15157.9
Ca I	315.1644	660000	13459	47036.23	15315.94
Ca I	375.0291	24000000	53229	47006.28	20349.26
Ca I	375.3364	85000	52871	47006.19	20371
Ca I	422.6728	6.54E+08	125725	23652.3	0
Ca I	428.3011	2.17E+08	20462	38551.56	15210.06
Ca I	430.7744	1.99E+08	25534	38417.54	15210.06
Ca I	442.5437	1.49E+08	18055	37748.2	15157.9
Ca I	458.1395	1.46E+08	21837	42170.56	20349.26
Ca I	468.5268	40000000	23366	44989.83	23652.3
Mg I	273.19937	20900000	7045	58442.88	21850.41
Mg I	276.52221		7265	58023.25	21870.46
Mg I	383.2299	202000000	60095	47957.06	21870.46
Mg I	383.82919	1130000000	66080	47957.05	21911.18
Mg I	389.8059	294000000	54449	83520.47	57873.94
Mg II	448.115	93000000	19821	93799.63	71490.19
Mg I	473.00286	1340000	10378	56186.87	35051.26
Mg I	804.772	1060000	10867	60263.58	47841.12
Mg I	805.4231	795000	10992	60263.58	47851.16
Mg I	809.8727	3230000	9626	60301.28	47957.06
N I	424.987	5180000	18292	120311.2	96787.68

depends on Ne and Te values.

In the case of non-H-like atoms quadratic Stark effect (two- and more-electron atoms which are called non-H-like) is dominant, the electron density (in cm^{-3}) could be determined from the FWHM of the line from the formula:

$$\Delta\lambda_{FWHM} \approx 2 \times 10^{-16} w\, N_e \quad (4)$$

Table 3
Impurities detected in polystyrene plasma.

Impurities	Wavelength (*nm*)
Al I	396.152
Si I	288.1577
P I	638.8579
Ca I	422.6728
Mg I	285.2126
N I	856.7
CH I	315.66
CN I	386.1, 388.34
C_2	469.5
H_2 I	406.688

where w is the electron impact parameter (Stark broadening value) which is a weak function of temperature [18].

The three elements in the polystyrene sample were taken into consideration for electron density measurements at wavelengths 247.8561 nm, 308.9 nm and 336.2 nm for C I, Al I and Ca I respectively. All the data points were fitted with Gaussian fitting function using the Origin software (version 8, Origin Lab Corporation, USA) to determine λ_{FWHM} (the wavelength of full width at half-maximum) of Ca is shown in Fig. 5.

Similarly, λ_{FWHM} for Al I and C I was determined. The Stark broadening values "W" were taken from GRIEM [20] at electron temperature of 10000 *K*. By inserting the values of λ_{FWHM} and the corresponding value of Stark broadening W in Eq. (4), the electron densities for C I, Al I and Ca I were calculated as listed in Table (5). Thus, the average value of the plasma density of polystyrene LIBS Plasma is $2.6 \times 10^{18} cm^{-3}$ and listed in Table (5).

It is important to mention that because the calculations for the electron temperature and the electron density have been carried out under the assumption that the plasma is at the local thermodynamic equilibrium LTE. So, we need to check the validity of the local thermodynamic equilibrium (LTE) assumption by applying the criterion given by McWhirter [21]. According to the criterion the lower limit for electron density for which the plasma will be in LTE is:

$$N_e\left(cm^{-3}\right) \geq 1.4 \times 10^{14} T^{1/2} (\Delta E)^3 \quad (5)$$

where T is the plasma temperature in eV, ΔE is the largest energy transition for which the condition holds. For C (I) it is ΔE = 7.68 eV, the highest temperature is 0.706 eV (8195.1 K), and its electron density lower limit value given by Eq. (5) is $5.32 \times 1016\ cm^{-3}$. The experimentally calculated density is greater than this value, thus the assumption that the plasma is in LTE is satisfied under the optimal conditions selected during the experiment.

4. Conclusion

In the present investigation, impurities of Al, Si, P, Ca, Mg, N elements in Polystyrene and Br, Mg, Ca and N in polycarbonate samples are identified. We have also detected molecular lines of CN, CO, C2 and CH in these samples. Presence of Al, Si, and P might be harmful to the human body. As the LIBS technique is useful for quick elemental analysis due to minimal sample preparation and cost effectiveness, therefore, it might be considered as a promising technology for the analysis of the fabricated materials in industry. It can be used to identify the impurities and hazardous elements in the materials during fabrication processes. The technique can also be used for plasma characterization of the materials.

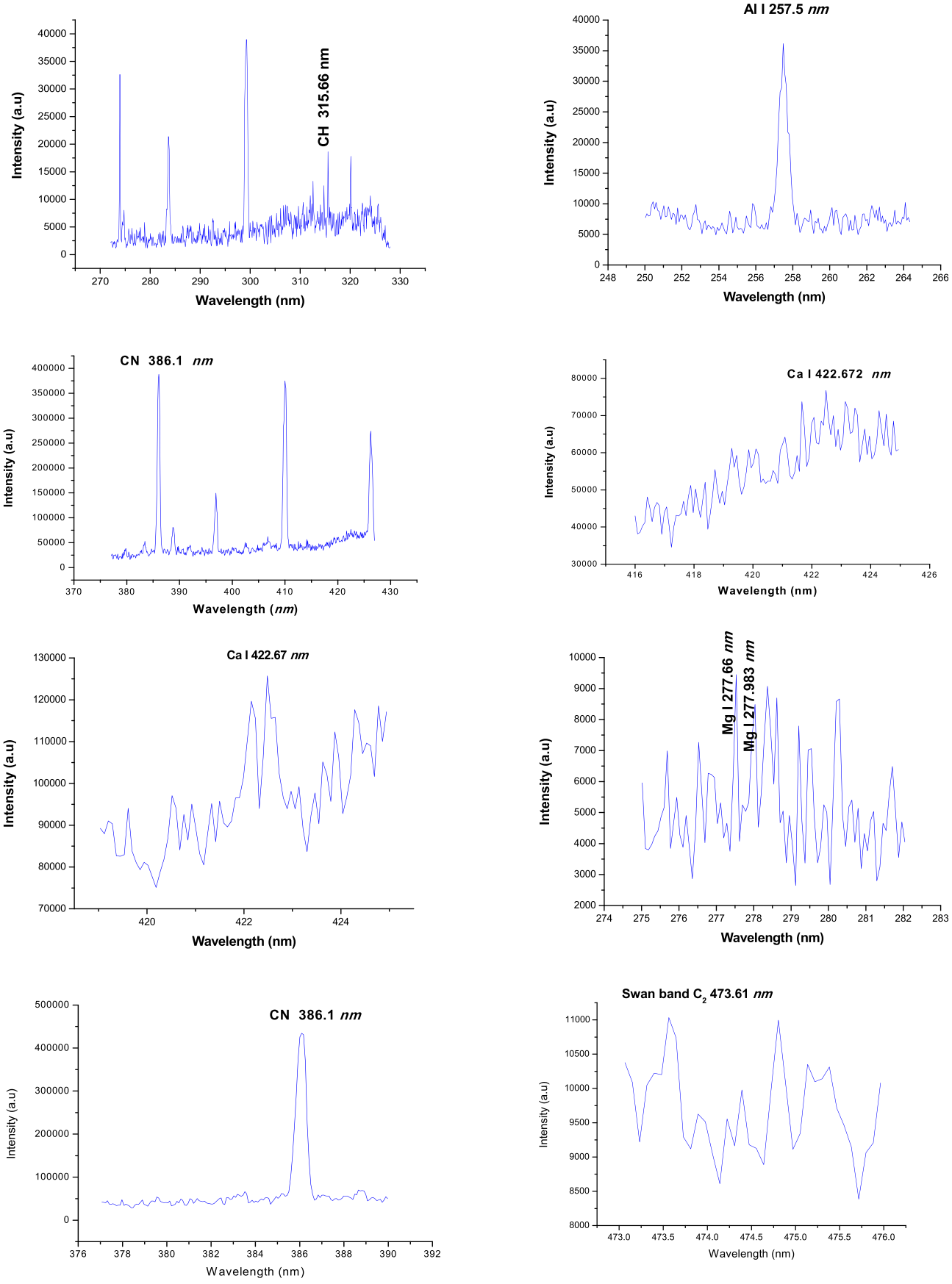

Fig. 3. (a) Impurity lines detected in LIBS Spectra of PS. (b) Impurity lines detected in LIBS Spectra of PC.

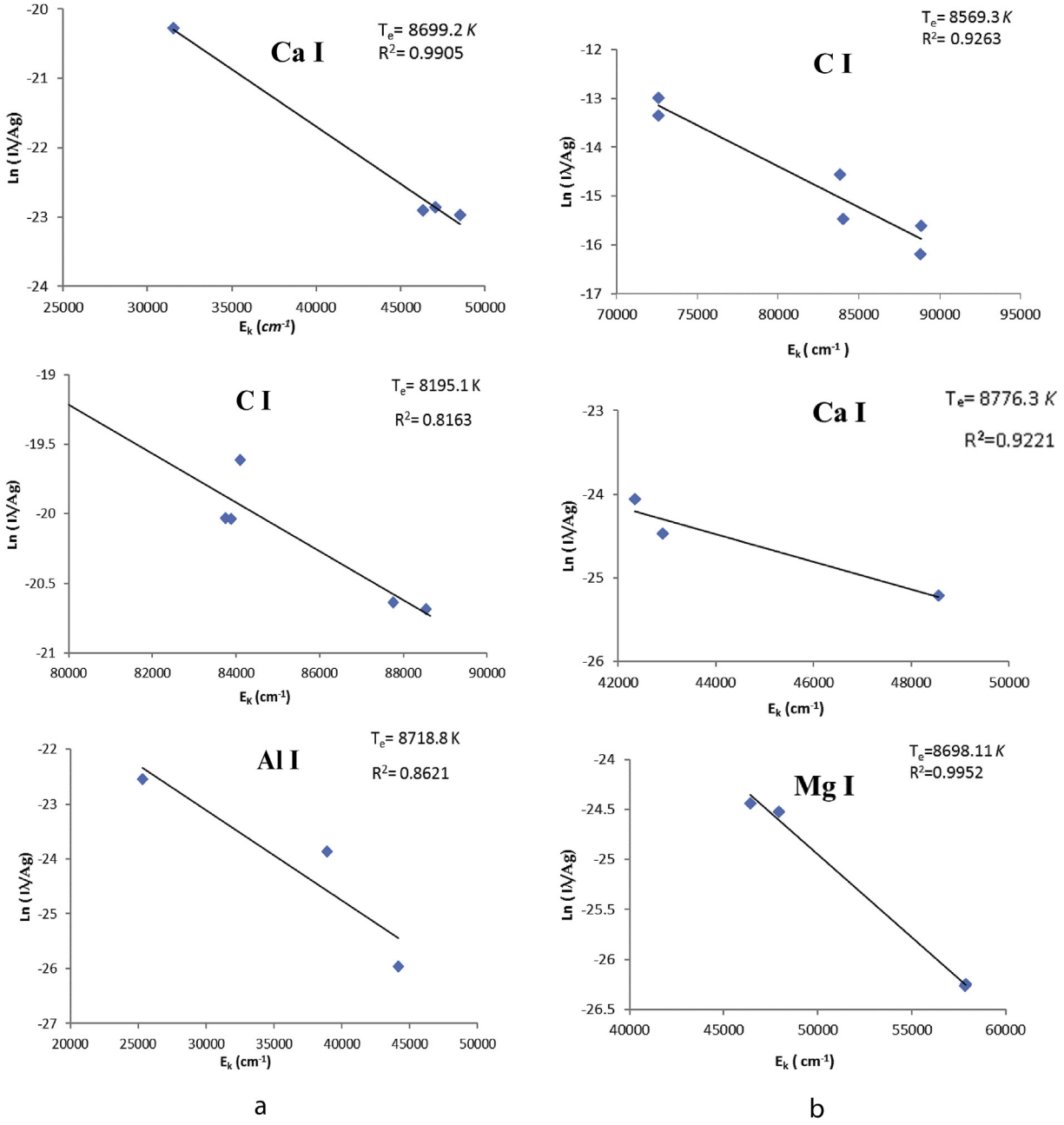

Fig. 4. (a) Boltzmann plot of polystyrene sample determined from the emission lines intensities of C I, Ca I and Al I. (b) Boltzmann plot of polycarbonate sample determined from the emission lines intensities of C I, Ca I and Mg I.

Table 4
Impurities detected in Polycarbonate plasma.

Impurities	Wavelength (*nm*)
Br I	679.004
N I	746.831
Mg I	383.829
Ca I	422.67
CN I	386.1
C_2	473.61

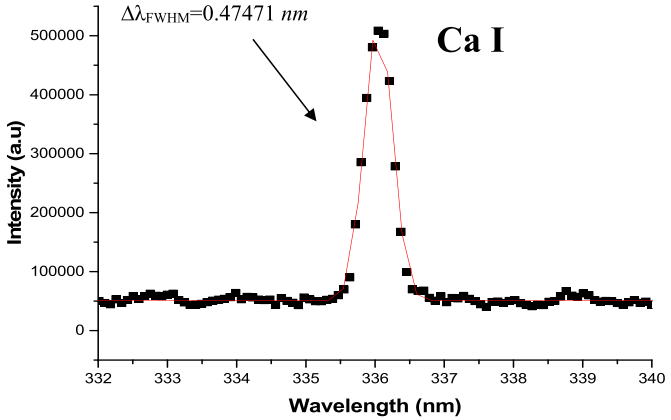

Fig. 5. Determination of λFWHM (the wavelength of full width at half-maximum) of Ca.

Table 5
The plasma electron density Ne determined from the observed C I, Al I and Ca I spectral lines in the polystyrene plasma.

Element	λ (*nm*)	*W* (*nm*)	2 W (*nm*)	$\Delta\lambda_{FWHM}$(nm)	N_e (cm^{-3})
C I	247.8561	3.61×10^{-4}	7.22×10^{-4}	0.54546	7.554×10^{18}
Al I	308.9	2.61×10^{-3}	5.22×10^{-3}	0.15402	2.95×10^{17}
Ca I	336.2	0.12	0.24	0.47471	1.97×10^{16}
Average $\mathbf{N_e}$					2.6×10^{18}

Acknowledgement

The authors are grateful to the Deanship of Scientific Research, King Saud University for funding through Vice Deanship of Scientific Research Chairs.

References

[1] L.J. Radziemski, D.A. Cremers, Laser-Induced Plasmas and Applications, Marcel Dekker, New York, 1989.
[2] A.W. Miziolek, V. Pallesschi, I. Schecchter, Laser-Induced Breakdown Spectroscopy, Cambridge University Press, Cambridge, MS, 2006.
[3] D.A. Rusak, B.C. Castle, B.W. Smith, J.D. Winefordner, Crit. Rev. Anal. Chem. 27 (1997) 257.
[4] Walid Tawfik Y. Mohamed, Opt. Laser. Technol. 40 (2008) 30.
[5] J. Sneddon, Y. Lee, Anal. Lett. 32 (1999) 2143.
[6] V. Majidi, M.R. Joseph, Crit. Rev. Anal. Chem. 23 (1992) 143.
[7] G.S. Senesi, M. Dell'Aglio, R. Gaudiuso, et al., Environ. Res. 109 (2009) 413.
[8] B. Rahid, S. Hafeez, N.M. Shaikh, M. Saleem, Int. J. Mod. Phys. B 21 (2007) 2697.
[9] W.A. Farooq, F.N. Al-Mutairi, Z.A. Alahmed, Opt Spectrosc. 115 (2013) 241.
[10] W.A. Farooq, F.N. Al-Mutairi, A.E.M. Khater, et al., Opt Spectrosc. 112 (2012) 874.
[11] C. Pasquini, J. Cortez, L.M.C. Silva, F.B. Gonzaga, J. Braz. Chem. Soc. 18 (3) (2007) 463.
[12] D.A. Cremers, L.J. Radziemski, Handbook of Laser-Induced Breakdown Spectroscopy, Wiley, West Sussex, UK, 2006.
[13] N.M. Shaikh, B. Rashid, S. Hafeez, Y. Jamil, M.A. Baig, J. Phys. D Appl. Phys. 39 (2006) 1384.
[14] S.L. Kakani, A. Kakani, Material Science, New Age International (P) Ltd, New. Delhi, 2004.
[15] D. William D, J. Callister, Materials Science and Engineering: an Introduction, John Wiley & Sons, Inc, USA, 2007.
[16] NIST National Institute of Standards and Technology, USA, Electronic Database, 2014. http://physics.nist.gov/PhysRefData/ASD/lines_form.html.
[17] A. Kramida, Y. Ralchenko, J. Reader, NIST ASD Team, NIST Atomic Spectra Database, 2014.
[18] G. Cristoforetti, G. Lorenzetti, P.A. Benedetti, E. Tognoni, S. Legnaioli, V. Palleschi, J. Phys. D Appl. Phys. 42 (2009) 225.
[19] S. Hafeez, N.M. Shaikh, M.A. Baig, Laser Part. Beams 26 (2008) 41.
[20] H.R. Griem, Plasma Spectroscopy, McGraw-Hill, New York, 1964.
[21] R.W.P. McWhirter, in: R.H. Huddlestone, S.L. Leonard (Eds.), Plasma Diagnostic Techniques, Academic Press, New York, 1965, pp. 201–264.